# Review on passive daytime radiative cooling: Fundamentals, recent researches, challenges and opportunities

Jay Prakash Bijarniya [a], Jahar Sarkar [a,*], Pralay Maiti [b]

[a] Department of Mechanical Engineering, Indian Institute of Technology (BHU) Varanasi, UP, 221005, India
[b] School of Material Science and Technology, Indian Institute of Technology (BHU), Varanasi, UP, 221005, India

## ABSTRACT

Passive radiative sub-ambient cooling is an emerging field of futuristic research and development and has the potential to reduce water and electricity demands, and the negative environmental effects of conventional cooling systems. Nighttime radiative passive cooling was achieved even long before, and daytime passive radiative cooling has gained recent momentum in cooling technology due to the development of metamaterials. In this paper, materials of passive radiative cooling are described with fundamental physics applied to the interaction between the material and electromagnetic wave and material design. Structure of material is an important parameter to achieve daytime radiative cooling and hence three major material structure categories (multilayer structure, porous polymer, and randomly distributed structure) are discussed. Subsequently, the various fabrication processes and characterization of metamaterials for daytime radiative cooling are also described. Effects of various environmental factors like ambient temperature, cloud cover, moisture, pollution, wind velocity on radiative cooling performances are also discussed. The potential applications such as water cooling, space cooling, power plant condenser cooling, solar panel cooling and spacecraft cooling are described. Finally, various challenges of daytime radiative cooling are discussed and subsequently, future recommendations are provided, which may be useful for further research and development in this field.

## 1. Introduction

Cooling is required for a wide range of domestic, commercial and industrial applications [1,2]. Conventional cooling involves consumptions of energy, water and/or synthetic chemicals. Hence in view of the following three major threads: (i) increasing demand for electricity (cooling system alone requires significant energy worldwide), (ii) water consumption and security, and (iii) negative environmental effect of synthetic working fluids, passive techniques are needed. Passive radiative cooling has the potential to provide the temperature lower than ambient without any energy or water consumption. It is also environmental-friendly due to zero-emission of $CO_2$ or other chemicals that are harmful to humankind. Conventional cooling devices reject heat to the air, water, etc., which ultimately yield local or global warming, whereas the passive radiative cooler rejects heat to the outer atmosphere and hence, no local/global warming. Passive radiative cooling can be considered as a renewable energy source, which can pump heat to cold space and make the devices more efficient than ejecting heat at earth atmospheric temperature. Passive radiative cooling is a method of

cooling objects with radiation energy exchange with cold outer space, which is at 3K. To exchange radiative heat with cold outer space, radiative cooler is required to emit radiation in atmospheric window 8–13 μm and reflect elsewhere, i.e., solar radiation and atmospheric radiation. Broadband spectrum emissive objects (very good in nighttime cooling) can absorb both atmospheric and solar radiations and hence it is very difficult to achieve daytime radiative cooling [3] and hence the spectrally selective emitter is preferable for daytime cooling.

The passive daytime radiative cooling (PDRC) was first proposed by Trombe [4] in 1967. Then the experimental setup to achieve daytime radiative cooling was fabricated from 1975 with the materials composition of metals and TEDLAR (polyvinyl-fluoride plastic) by a shielded radiator from direct sun radiation but worked well only for nighttime cooling [5]. There were some subsequent developments of radiative cooler such as coated thin solid film on an aluminum substrate with $SiO_{0.6}N_{0.2}$ [6] and double layers of $SiO_2$ and $SiO_{0.25}N_{1.52}$ on Al substrate having higher value of the complex refractive index in order to achieve a selective spectrum [7] but was not successful. A clear sky can work as a heat sink for strongly emitting devices in an 8–13 μm wavelength

spectrum, also called the atmospheric window. Hence, some research works are available on the development of such coated material and the effect of various parameters related to material such as surface emissivity, atmospheric radiation, surface orientation and local climate [8–11]. For daytime radiative cooling, reflectivity or non-absorptivity of the surface also has higher consideration to achieve less solar heat gain and this succeeded in the 2010s by the development of photonic materials made of surface phonon resonant nanoparticles [12] or multilayer nanostructure [13]. The first numerically developed daytime photonic multilayer structure consists of a dielectric reflector made of a combination of high index ($TiO_2$)-low index ($MgF_2$) dielectric material on a silver substrate and 2D planer structure of SiC and quartz [13]. The daytime radiative cooling was experimentally achieved by Raman et al. [14] in 2014 and their development boosted up the research on this area.

Several review papers have been published in the last five years on radiative cooling [15–24], which are consisting of fundamental energy interactions of the cooler surface with solar and atmosphere [16–24], historical development of passive radiative cooling [16], photonic material structure, category and properties [19–21,23], prototype development [17,18], prospects and various nighttime and daytime cooling applications [15,16,19,22,23]. However, electromagnetic wave interactions with material surface, environment effect and challenges have not been discussed, which are fulfilled in this paper. Hence, the fundamental physic (electromagnetic wave interaction) is described in Section 2 with radiation energy exchange analysis. Section 3 elaborates on the material characterization and categorization with layered, pigmented and porous polymer with fabrication methods. Section 4 deals with the effect of environmental conditions (humidity, wind speed, pollution, etc.). Section 5 contains various applications to report performance and associated challenges of the radiative cooler. Specific contributions are (i) electromagnetic wave and material interaction with equations, which is needed to simulate and optimize PDRC material for required surface emissive properties, (ii) environmental effect, which is needed to predict the feasibility of PDRC in the certain climatic zone. Finally, conclusions and research recommendations are provided based on the literature review.

## 2. Fundamentals and analysis

### 2.1. Fundamental physics

The blackbody radiation spectrum described by Plank's law is given in Eq. (1). A blackbody radiates with the emissivity of unity covering broadband of spectrum; however, a blackbody is not suitable for radiative cooler because of atmospheric radiation outside 8–13 μm range get absorbed, requires the development of selective emissive surfaces [25].

$$I_B(T, \lambda) = \frac{2hc^2}{\lambda^5 \left( e^{\frac{hc}{\lambda kT}} - 1 \right)} \qquad (1)$$

Where, $I_B(T, \lambda)$ is blackbody emissive power, h is Plank's constant, c is the speed of light, k is Stephan Boltzman constant, λ is the wavelength, and T is the absolute temperature.

Hence, in order to make radiative cooler optimized, the ideal selective surface needs to be introduced, which is emissive in the atmospheric window only and reflective elsewhere. The surfaces which are emissive outside the atmospheric window also absorb radiation from atmospheric emission. Fundamentals required by ideal selective surfaces need an introduction study of material and radiation. Radiation here is considered as an electromagnetic wave, which is a suitable assumption to study emission and reflection; however, photon nature also needs to be considered if considered material has a bandgap near to photon energy [16]. The electromagnetic waves and material interaction described by

Maxwell's equations [26]:

$$\nabla \times \vec{E} + \frac{\partial \vec{B}}{\partial t} = 0 \qquad (2)$$

$$\nabla \times \vec{H} - \frac{\partial \vec{D}}{\partial t} = \vec{J} \qquad (3)$$

$$\nabla \cdot \vec{B} = 0 \qquad (4)$$

$$\nabla \cdot \vec{D} = \rho \qquad (5)$$

$$\vec{D} = \varepsilon \vec{E} = \varepsilon_0 \vec{E} + \vec{P} \qquad (6)$$

$$\vec{B} = \mu \vec{H} = \mu_0 \vec{H} + \vec{M} \qquad (7)$$

Where, E and H are electric and magnetic fields, respectively. D and B electric and magnetic charge displacement, respectively. $\varepsilon_0, \mu_0$ are permittivity and permeability of a vacuum. P and M are polarization and magnetization of the material. $J, \rho$ are free current and charge density.

The above-described Maxwell's equations are difficult to solve analytically and hence the numerical method is used to solve for the selected material and radiation spectrum domain. The numerical solution has many forms like TMM, FDTD, RCWA, etc. depending on time domain, frequency domain, geometry, assumptions, and approximations [27–30].

A mismatch between the refractive index causes scattering of light in material and backscatters for the slab thickness. For incident radiation at angle $\theta_i$ and propagation through the medium of refractive index $n_1$ to another medium $n_2$, the reflection coefficient for s-polarization is given by Ref. [31].

$$r_s = \frac{n_1 cos\theta_i - n_2 sin\theta_t}{n_1 cos\theta_i + n_2 sin\theta_t} \qquad (8)$$

and for p-polarization,

$$r_p = \frac{n_2 cos\theta_i - n_1 sin\theta_t}{n_2 cos\theta_i + n_1 sin\theta_t} \qquad (9)$$

Where $\theta_t$ is the angle from normal in medium 2(transmission side).

The reflectivity for s and p-polarization respectively given by:

$$R = |r_s|^2 \text{ and } R = |r_p|^2 \qquad (10)$$

From the above equations, it is clear that any change in refractive index leads to some reflection and this concept can be utilized for maximum reflection of varying refractive index alternatively in dielectric stack multiple layers. Multilayer media can be modeled by the transfer matrix method [32] and optimized by the needle optimization method [33]. Various algorithms were developed to optimize the thin-film multilayer optical structure that applied to the thermal broadband application, which includes jump method, spiral search method, needle optimization and evolutionary algorithms [34]. Taguchi's method was also used to optimize the multilayer photonic structure and found comparable to the stochastic optimization technique [35].

Other than layered media, randomly distributed particles scatter the light and lead to diffuse reflection or backscattering. $SiO_2$ microsphere of d = 0.9 μm in diameter with a fill fraction 0.55–0.64 backscatter the light without absorption. From a single particle scattering, Mie theory, which is also a derived form of Maxwell's equations used to apply and mathematical formulation [36] is given in Eqs. (11)–(14).

$$R = \left| \frac{1 - \sqrt{\varepsilon_e / \mu_e}}{1 + \sqrt{\varepsilon_e / \mu_e}} \right|^2 \qquad (11)$$

Where, $\varepsilon_e$, $\mu_e$ are effective permittivity and permeability of embedded

particle medium. The $\varepsilon_e$, $\mu_e$ can be expressed in the form of particle radius $a$ and wavelength $\lambda$ and for small pigment volume fraction $f$ and it is given as:

$$\varepsilon_e = \varepsilon_m \left[ 1 + i \frac{3f\lambda^3}{16\pi^3 a^3} (S1(0) + S1(\pi)) \right] = \varepsilon_m(1 + \gamma) \qquad (12)$$

$$\mu_e = 1 + i \frac{3f\lambda^3}{16\pi^3 a^3} (S1(0) - S1(\pi)) = 1 + \delta$$

$\varepsilon_m$ is the permittivity of medium alone in which particle is pigmented (13)

$$S1(\theta) = \sum_{n=1}^{\infty} \frac{2n+1}{n(n+1)} \left[ \alpha_n \frac{\mathscr{P}_n^1(cos\theta)}{sin\theta} + \beta_n \frac{d}{d\theta} \mathscr{P}_n^1(cos\theta) \right] \qquad (14)$$

Where S1(θ) is angle-dependent scattering amplitude function. $\alpha_n$, $\beta_n$ are scattering coefficients and expressed as Ricatti-Bessel function. $\mathscr{P}_n^1$ is a Legendre polynomial of order n and degree unity. For higher pigment volume fraction, $\varepsilon_e$, $\mu_e$ can be expressed based on Maxwell-Garnett theory as:

$$\varepsilon_e = \varepsilon_m \frac{1 + 2\gamma/3}{1 - \gamma/3} \qquad (15)$$

$$\mu_e = \frac{1 + 2\delta/3}{1 - \delta/3} \qquad (16)$$

High dielectric constant material reflects the corresponding spectrum because the dielectric constant is a function of wavelength [37]. Pigmented foil enhances dielectric constant and strongly backscatters spectrum comparative to the size of pigmented particles. $TiO_2$ of size 0.23 μm, dispersed in polyethylene as lossless material, can backscatter sun radiation and allow the transmission of larger wavelengths in the atmospheric window [36]. Backscattering is also an option similar to a reflection in PDRC material. Backscattering can be achieved through high concentration (40–50%wt) of titania and silica particles in paint or coating [38]. Several potential pigments like $TiO_2$, $ZrO_2$, ZnS, ZnSe, and ZnO tested with pigment fraction of 0.10–0.15 in polyethylene of 400 μm thickness. ZnS gave better results for radiative cooling properties. $TiO_2$ has better solar reflectivity but absorbs UV radiation due to bandgap overlap and $ZrO_2$ lossless in UV but lower refractive index so reflects less than titania [39].

Simulation done by Mandal et al. [40] showed that porous polymers have excellent backscattering capabilities with the porosity of 50–500 nm for solar light. The backscattering due to porosity also experimentally substantiated by photon mean free path 6 μm for blue and 10 μm for NIR wavelengths. However, homogeneous solid polymers surface gets heated due to absorption in 300–420 nm wavelength range because of the presence of C–C, C–O, and C–H bond [38,41,42].

Finally, it can be concluded that multilayer, randomly particle distributed and porous polymer metamaterial structures are suitable for passive day time radiative cooling surfaces. Multilayer structures require high reflective metals at the bottom and only silver can reflect 97% in metal; however, randomly distributed and porous polymer designed to perform without the need of silver and even substrate independent [43].

### 2.2. Energy analysis

The ideal radiative cooler decoupled from the atmosphere can achieve equilibrium temperature of outer space, i.e., 3K, but the actual theoretically limit by considering atmospheric radiation and suppressing parasitic heat gain attain an average 37 ℃ below ambient in Ref. [44]. The more actual scenarios have humidity and cloud in the environment and need consideration. Han et al. numerically and experimentally studied the performance of two types of radiative cooler, photonic and enhanced specular reflector (ESR) film in Singapore climatic conditions. Both the coolers were unable to achieve below ambient temperature during clear sky condition; however, ESR was sub-ambient during a cloudy day because of higher emissivity in the atmospheric window [45]. Yuan et al. [46] fabricated highly emissive five layers of the lossy material based radiative cooler, which also have emissivity outside the atmospheric window and theoretically with a back metal reflector remain sub-ambient during the daytime, because of higher emission in atmospheric and as well net emission in the outside atmospheric window. The ideal radiative cooler has emissivity as one in the atmospheric window and zero in outside, or reflective outside 8–13 μm range. A numerical study showed that a pyramidal multilayer nanostructure has near-ideal properties with $Al_2O_3$ and $SiO_2$ alternating layers [47].

Various heat transfer interactions with the radiative cooler are illustrated in Fig. 1. For the surface temperature of $T_s$, the cooling power, $P_{cool}(T_s)$ is given by Ref. [14,45],

$$P_{cool}(T_s) = P_{rad}(T_s) - P_{atm}(T_{amb}) - P_{solar} - P_{conv+cond}(T_s, T_{amb}) \qquad (17)$$

where,

$$P_{rad}(T_s) = 2\pi \int_0^{\frac{\pi}{2}} \sin\theta \cos\theta \int_0^{\infty} I_B(T_s, \lambda)\varepsilon(\lambda, \theta)d\theta d\lambda \qquad (18)$$

$$P_{atm}(T_{amb}) = 2\pi \int_0^{\frac{\pi}{2}} \sin\theta \cos\theta \int_0^{\infty} I_B(T_{amb}, \lambda)\varepsilon(\lambda, \theta)\varepsilon_{atm}(\lambda, \theta)d\theta d\lambda \qquad (19)$$

$$I_B(T, \lambda) = \frac{2hc^2}{\lambda^5 \left( e^{\frac{hc}{\lambda kT}} - 1 \right)} \qquad (20)$$

$$\varepsilon_{atm}(\lambda, \theta) = 1 - t(\lambda)^{\frac{1}{\cos\theta}} \qquad (21)$$

$$P_{solar} = \int_0^{\infty} I_{solar}(\lambda)\varepsilon(\lambda, \theta_{solar})d\lambda \qquad (22)$$

$$P_{conv+cond}(T_s, T_{amb}) = h_c(T_{amb} - T_s) \qquad (23)$$

ε(λ,θ) is the spectral and angular emissivity of a radiative cooler. Atmospheric transmittance is t(λ) and $\varepsilon_{atm}(\lambda, \theta)$ is atmospheric emissivity depend upon wavelength and zenith (θ), $h_c$ combined convection and conduction heat transfer coefficient.

Calculation of emissivity is based on reflectivity for opaque surfaces, which is given by the following [48],
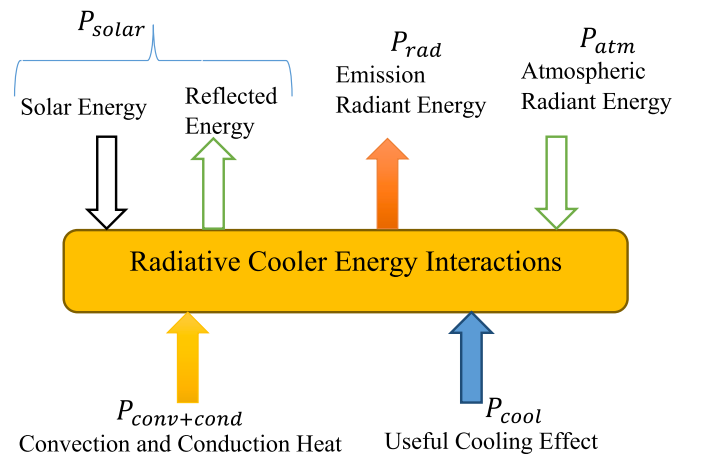


**Fig. 1.** Energy balance of a passive radiative cooler.

$$\alpha(\lambda) + \rho(\lambda) = 1 \tag{24}$$

$$\varepsilon(\lambda) = \alpha(\lambda) \tag{25}$$

Where, $\alpha(\lambda)$, $\rho(\lambda)$ *and* $\varepsilon(\lambda)$ are specular absorptivity, reflectivity, and emissivity, respectively. For the given surface properties and environmental conditions, the cooling capacity of the cooler can be evaluated based on the above formulations.

## 3. Material processing and characterization

Manufacturing of radiative cooling surface requires a wide range of techniques from E beam evaporation of base material to simply spraying of a chemical solution on a substrate. Layer material of nanometer thickness requires high precision machines and high costs but was first to achieve day time radiative cooling [14]. However, porous polymer and randomly distributed microsphere are a potential alternative to layer medium for the same performance and also easy to fabricate [40, 49]. In Fig. 2, the structural construction is represented for all the three types of radiative cooling surfaces, i.e., multilayer, randomized particle and porous polymer structure. Fig. 3 illustrates the example of the spectral behavior of these three developed materials measured in 0.2 µm–15 µm range using respective instruments for UV-VIS, Near-IR and Mid-IR as described below.

Characterization of optical properties of radiative cooler requires measurement of wavelength from 0.2 to 20 µm range, and this is usually done in two segments by FTIR for MIR and UV–Vis spectrophotometer for visible to NIR spectrum. With these instruments integrating sphere as an accessory requires in order to take account of all reflection and emission, i.e., diffuse and specular [50]. However, for specular and angular reflection, the ellipsometer and angular specular reflectance accessory are used to interface with the instrument [14,40,51]. Fabrication and characterization of PDRC materials: (i) layered (ii) Porous and (ii) Random distributed and pigmented materials are discussed in detail.

### 3.1. Multi-layer media structure

Layered media with PDRC properties was developed by Raman et al. [14] consisting of seven layers of alternating $HfO_2$ and $SiO_2$ on the top of 200 nm Ag layer, and the substrate used was silicon wafer with Ti as an adhesive. The structure was optimized by using the needle optimization technique and that is most prominent in coating optimization [33]. In continuation of the above layered PDRC, several other materials with a different number of layers were developed by the researchers [44, 52–57]. Detailed comparison of parameters like materials, temperature
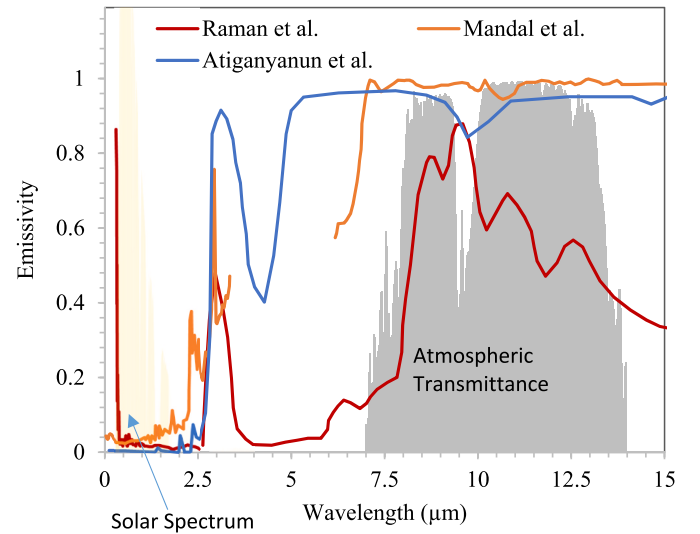


**Fig. 3.** Emissivity spectrum of multilayer structures (Raman et al. [14]), random particle distributed in the matrix (Atiganyanun et al. [49]) and porous polymer structure (Mandal et al. [40]) radiative cooling surfaces in UV-VIS-NIR and MIR.

drop and manufacturing methods for layered material is shown in Table 1.

A relatively simple photonic cooler was developed by Kou et al. [53] consisting coated silver layer of 120 nm on a fused silica substrate of 500 µm thick and a top layer with 100 µm thickness PDMS. Their broadband emitter is shown better results than selective emitter for higher energy flux because of the partial absorption of atmospheric radiation; however, for a higher temperature drop, selective emitter is suitable. Chen et al. [44] computed the fundamental limit of cooling temperature is 60ºC at the earth, with the emissivity of material matched with the atmospheric window. By combined photonic and thermal design, they experimentally achieved 42ºC temperature reduction under peak solar radiation. Their photonic structure consists of $Si_3N_4$, amorphous Si, Al of 70, 700, and 120 nm, respectively, and thermally insulated from the atmosphere to reduce parasitic heat loss due to convection by creating a vacuum around the radiator. Gao et al. [56] manufactured a PCSUVA (Photonic crystal structured UV curable adhesive) on PET (Polyethylene terephthalate) substrate by UV nanoimprint lithography for above ambient PDRC which applies to PV panel cooling. An FDTD simulation was performed in order to calculate reflectivity and emissivity of material and 3% difference was observed
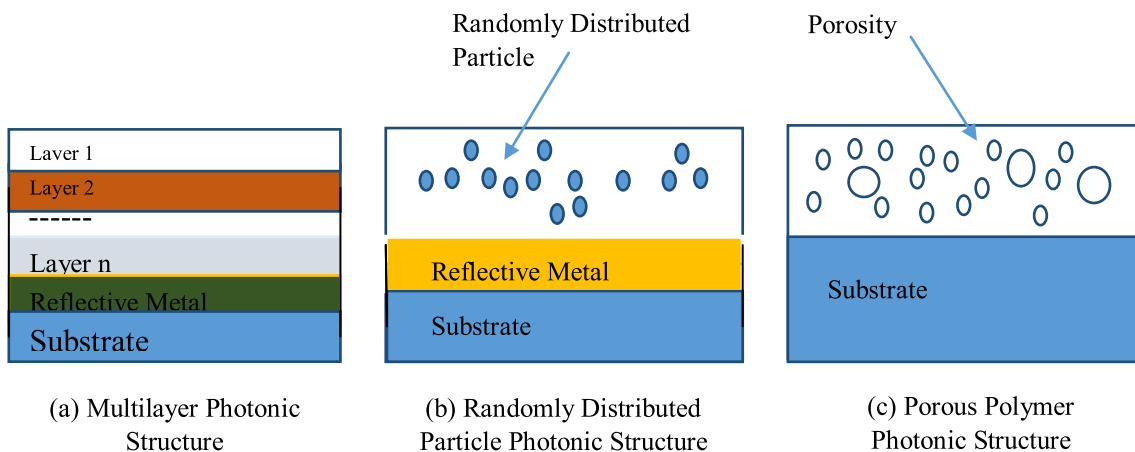


**Fig. 2.** Different material structures for daytime radiative cooling.

**Table 1**
Layered material comparison for PDRC.

| Authors [Reference] | Layer materials | Manufacturing method | Temperature drop | Remarks |
|---|---|---|---|---|
| Raman et al., 2014 [14] | $SiO_2$, $HfO_2$, Ti, Ag, Si | E Beam Evaporation | 4.9°C | Dry weather experimental condition |
| Gentle and Smith, 2015 [43] | Vikuiti Enhanced specular reflector, Ag | Sputter coating | 2°C | Sydney dry weather |
| Chen et al., 2016 [44] | $Si_3N_4$, Si, Al, ZnSe | E Beam Evaporation (Al, Si), High-density Plasma CVD ($Si_3N_4$) | 42°C | Dry weather experimental condition |
| Kou et al., 2017 [53] | PDMS, Ag, Silica wafer | E Beam Evaporation (Ag) Spin Coating (PDMS) | 8.2°C | California weather |
| Lee et al., 2018 [55] | $Si_3N_4$, $SiO_2$, Ag | E Beam Evaporation | 3.9°C | Wearable's color devices |
| Gao et al., 2019 [56] | PET, PCSUVA, Si | UV nano-imprint lithography | 7.7°C (Reduction, above ambient) | Shanghai China, Angle independent |
| Jeong et al., 2020 [3] | $SiO_2$,$TiO_2$, Ag | E Beam Evaporation | 7.2°C | Hong Kong, Humid climate |
| Cunha et al., 2020 [57] | Al, $SiO_2$, SiNx, $TiO_2$ | Dc magnetron Sputtering | 2.5°C | Winter Climate |

due to density difference of fabricated layers. Jeong et al. [3] developed a radiative cooler with extensive FDTD optimization of thickness, the ratio of thickness and number of layers of $SiO_2$ –$TiO_2$ alternating. They found 35% enhancement of emissivity over $SiO_2$ –$HfO_2$ photonic layer media with a slight decrease (0.03) in reflectivity, which ultimately results in 136.3 W/m$^2$ cooling flux i.e. 90 W/m$^2$ higher than $SiO_2$ –$HfO_2$ combination, subsequently a drop in cost was observed due to $TiO_2$ is cheaper by half than $HfO_2$ and overall 17% decrement in cost from 70 $/m$^2$ to 58 $/m$^2$ [3]. Additionally, manufacturing by fast alternating sputtering was demonstrated for $SiO_2$ –$TiO_2$ thin amorphous film with a controlled refractive index emphasis on the use of $TiO_2$ in combination with Silica [58,59]. Cunha et al. [57] developed a multilayer structure based on optical constants (refractive index [60] and extinction coefficient) with optimized six layer stack of Al/$SiO_2$/SiNx/$SiO_2$/$TiO_2$/$SiO_2$ on silicon or glass as a substrate, with an average reflectivity of 88% without silver coating.

Gentle et al. [44] concluded that two or more polyesters on a silver layer could lead to a surface sub-ambient during a hot summer day. 300 number layer of polymer with an average thickness of 110 nm over the Ag layer deposited the coextruded combination of many bilayers. The bilayers have a high index-low index combination to act as a polymer mirror, which is reflective in the 0.3–1.0 μm range and transmit NIR spectrum, which is further reflected by the silver layer. The silver layer reflects in both NIR and MIR regions and supports the MIR emission of polymers toward the sky. Pech-May and Retsch [61] numerically proposed an angle selective low-pass filter for reflection of the entire solar spectrum and transmission of mid-infrared radiation on a nocturnal passive radiator. Their low-pass filter consists of multiple layers of Bragg stack with different periodicities and performs well for incident angle 23° and larger. Shahsafi et al. [62] also developed void and silica-based wide-angle spectrally selective absorber/emitter. Fan et al. numerically evaluated the daytime cooling performance of proposed radiative cooler consisting multilayer of yttria-stabilized zirconia, glass ($SiO_2$) and silver

and achieved a net cooling flux of 95.1 W/m$^2$, a reduction in temperature 10°C and 6°C below ambient under 1m/s and 3 m/s wind speed respectively [63]. The most developed cooler have the silvery appearance which is aesthetically less appealing in certain applications, a metal-insulator-metal (MIM) structure under a selective emitter can exhibit colors with a very low dip in reflectivity. The thin-film resonator composed of MIM can produce colors like cyan, magenta, and yellow on the silvery background, and selective emitter consists of $Si_3N_4$, $SiO_2$ of 910 nm and 650 nm respectively optimized using rigorous coupled-wave analysis (RCWA) [12] and transfer matrix methods [57]. The other $Si_3N_4$/$SiO_2$ multilayer photonic radiative cooler was fabricated using impedance mismatch in the refractive index in the solar spectrum and phonon resonance in MIR spectrum [64]. Cooling performance of 87 W/m$^2$ was observed for these structures. Yang et al. [65] proposed a bulk material of lithium fluoride crystal on silver backing based radiative cooling, which has simple to coat than thin films and achieved 5 °C below ambient cooling performance.

### 3.2. Porous polymer structure

A comparison of various developed porous polymer PDRC materials is shown in Table 2 [40,66–69]. Fabrication of multilayer photonic structure is still costlier and difficult to commercialize, therefore despite high efficiency, layered PDRC is used to compare with cool roof paints (CRP). Cool roof paints have embedded with $TiO_2$ and ZnO, which absorb the UV portion of the solar spectrum and reduce the solar reflectivity to 0.85. Inspired from CRP, Mandal et al. [40] created a low-cost porous material similar to PRC and replaced $TiO_2$ and ZnO with nano-voids with the size range of 50–500 nm that have a high backscattering of sunlight and achieved net cooling during the day. In other studies, both indoor and outdoor experiment conditions with PDMS/metal (Al and Ag) structure was performed. The PDMS/metal structure fabricated using solution coating; however, porosity is not

**Table 2**
Porous polymer PDRC material comparison.

| Author [Reference] | Porous structure materials | Manufacturing method | Cooling performance | Remarks |
|---|---|---|---|---|
| Mandal et al., 2018 [40] | P(VdF-HFP)$_{HP}$, any Substrate | Spray Coating Painting | 6°C Below Ambient | Tested for USA and Bangladesh |
| Peng et al., 2018 [67] | HDPE | Extrusion | 2.3°C (Skin Temperature) | Product wearable fabric |
| Zhou et al., 2019 [66] | PDMS | Solution-based rolled to rolled | Sub-ambient | New York climate, Scalable manufacturing |
| Li et al., 2019 [68] | Wood | Delignification, densification | 4 °C Below Ambient | Product from wood with high strength used as roof structure |
| Wang et al., 2020 [69] | PVDF, $SiO_2$ microsphere, tetraethyl orthosilicate | Electrospinning | 6°C below ambient | Experimented at China, Scalable manufacturing |

**Table 3**
Random and pigmented material structure comparison for PDRC.

| Author [Reference] | Random Structure Materials | Manufacturing Method | Cooling Performance | Remark |
|---|---|---|---|---|
| Bao et al., 2017 [78] | $SiO_2$, $TiO_2$, SiC, Al | Spray Coating | 5°C Below Ambient | Humid weather condition, China |
| Zhai et al., 2017 [32] | $SiO_2$, Ag | Embedded in polymer by rolling | 93W/m² Cooling Power | Arizona clear sky day experimental condition |
| Huang et al., 2017 [79] | Acrylic resin, $TiO_2$, carbon black | Embedded in acrylic resin | 100W/m² Cooling Power | |
| Atiganyanun et al., 2018 [49] | $SiO_2$ | Spray Coating | 7°C Below commercial cool paint | New Maxico climate |
| Ao et al., 2019 [48] | $NaZnPO_4$, Al | Spray Coating | 1.5°C Below Ambient | Beijing field test |

given importance; instead, a metal (Al or Ag) is used for reflection; PDMS is emissive in mid-infrared regime after a thickness of 100 μm makes it a promising material for daytime radiative cooling. The suppression of solar heat is the most important technical issue for practical daytime cooling and a beaming system integrated here to block the solar radiation and achieved the radiative/emissive surface sub-ambient throughout the day-night cycle. The angle of the radiator in indoor conditions varied from 15° to 90° and a temperature drop of 2 °C to 9.5 °C obtained [68]. Polyester has potential as a mirror in the visible spectrum, and with a silver backing, it reflects whole solar spectra; this combination was tested for sub-ambient throughout the day for a ten-day experiment by Gentle et al. [43].

Peng et al. [67] fabricated a porous polymer structure of porosity ranging from 100 nm to 1000 nm by the extrusion method. A mixture of polymer, i.e., HDPE and paraffin oil, is made in the weight ratio of 3.5:1 as optimized and heated to 180°C then extruded as thin fiber. After cooling of extruded structure removal of paraffin oil leaves nano porosity in microfibers, which make it possible for a photonic structure reflecting visible spectrum and transmitting IR wavelengths, they fabricated this structure for emphases on the wearable with the potential of large scale industrial production. However, comparing with Mandal's work, it is possible to create a porous structure with continuous surface and possible utilization for a wide variety of applications. The polymers are sustainable to environmental changes and resistant to damage with weather conditions with flexibility and mechanical strength, making them a potential material for further research on radiative cooling and an added advantage of low cost and easy to fabricate [70]. Li et al. [68] developed a radiative cooling surface by delignification and densification of natural wood. The delignification creates and leaves disordered mesoporous cellulose and randomized fabric, which strongly backscatters the solar spectrum. The emission in the mid-infrared zone is due to molecular vibration and stretching of cellulose makes it possible for day time radiative cooling. They achieved a temperature reduction of 4 °C from ambient during the daytime experiment, and the measured reflectivity 96% with emissivity in the mid-infrared zone is above 0.9. The additional advantage of wood as radiative cooling is the direct application in building and densification of cooling increased the total strength of eight fold than natural wood. Wang et al. [69] produced a film of PVDF/tetraethyl orthosilicate of 300 μm thickness, which has above 97% solar radiation reflectivity without any silver coating due to nanopores in developed structure (presence of $SiO_2$ microsphere emits in the atmospheric window with an average emissivity of 0.96). Some researchers fabricated photonic radiative cooler, inspired by the Saharan ant, which has high reflective skin in solar spectrum and emission in the atmospheric window and achieved 80–144 W/m² cooling performance in varied climate conditions [71,72].

### 3.3. Random and pigmented media

Randomly distributed lossless material used to radiate the selective spectrum in the atmospheric window leads to PDRC, which can be made by an easy fabricate technique. Table 3 shows the comparison of nanoparticle and microparticle randomly distributed layers in order to achieve cooling in the day time [12,73–79]. Bao et al. [12] developed a theoretical model from the combination of two nanoparticle $SiO_2$ + SiC and $TiO_2$ + SiC on Al and black painted Al and shown 5°C drop in temperature during daytime, however during experiment it not achieved because of high (55%) humidity location. Gentle and Smith choose $SiO_2$ + SiC nanoparticles of size 50 μm in a 25 μm thick PE sheet backed by Al. The $SiO_2$ and SiC have phonon resonance peaks lies in the range of 8–10 μm and 10.5–13 μm, respectively, makes it possible to emit in atmospheric window simultaneously avoiding ozone IR peak. Zhai et al. [32] experimentally demonstrated $SiO_2$ microsphere-based daytime radiative cooling with a peak of 93W at noontime, embedded in polymethyl-pentene. These particles emit in the atmospheric window due to phonon enhanced Fröhlic resonance of microsphere. The complex refractive index of the particles embedded system is given by,

$$n + ik = \sqrt{\mu_{eff} \cdot \varepsilon_{eff}} \tag{26}$$

Effective permittivity, $\varepsilon_{eff} = \varepsilon_p[1 + i\gamma(S_1 - S_2)]$ $\tag{27}$

Effective permeability, $\mu_{eff} = \mu_p[1 + i\gamma(S_1 - S_2)]$ $\tag{28}$

$$\gamma = \frac{3f}{2(k_0 a)^2} \tag{29}$$

Where, $k_0$ is the free space wavenumber, $\varepsilon_p, \mu_p$ are single particle, permittivity and permeability respectively, $f$ is filled factor, and $S_1$, $S_1$ are forward and backward scattering coefficient of the individual microsphere.

Atiganyanun et al. [49,77] developed a random structure of $SiO_2$ microparticles to coat on a black substrate the randomized silica particles strongly scatters the solar spectrum and facilitates the emission of the mid-IR spectrum. Spray coating deposition further emphasized that these structures have strong commercial potential as radiative cooling. Huang et al. [79] proposed a double-layer coating photonic structure embedded with nanoparticles of titanium oxide in rutile form and carbon black for solar spectrum reflection and emission in the atmospheric window, respectively. The nanoparticle embedded in acrylic resin layers of 500 μm thickness with a low particle volume fraction of 4%. Their structure gets optimum result at 0.2 μm size of $TiO_2$ nanoparticle for a maximum reflectivity of solar radiation, which corresponds to 0.91 and emissivity in the atmospheric window is 0.95. Fast manufacturing by the roll to roll method for particles embedded in TPX (polymethyl-pentene) can achieve for day time radiative cooling technology, randomly distributed microsphere in TPX backed by silver for solar spectrum reflectance and $SiO_2$ have strong phonon polariton resonances at 9.7 μm which is responsible for emission at this wavelength [32].

Photonic and amorphous structures used to experience sub-ambient diurnal cooling and pigmented foil as a solar spectrum reflective layer applied to cool underlying objects [39]. These pigmented foils with ZnS or ZnO further coated with thin-film PbS by chemical solution deposition and have enhanced cooling properties. Reflection of the solar spectrum can be made through low band semiconductors and significant

dielectric constant, like Te (0.32eV), PbS (0.37eV) and PbSe (0.27eV) which are transparent for mid-infrared spectrum as well [74]. Te generally deposited through vacuum evaporation method, but a simplified method suggested by Engelhard T et al. through electrochemically and get similar properties as vacuum evaporation deposited [73]. Ao et al. fabricated two different radiative coolers, specular with Ag and diffuse $Na_2ZnPO_4$ reflectors on polished Al substrate and achieved net radiative cooling for both. They selected $Na_2ZnPO_4$ over $TiO_2$ due to its higher reflectivity in the NIR spectrum [76] and spray deposited on Al substrate a solution in a 1:3 vol ratio of sodium zinc phosphate stirred for 30 min at a rate of 300 r/min in isopropyl alcohol. The cost is lower for diffuse radiator due to its easy to fabricate technology and its estimates around 10\$/m$^2$; however, for specular, it is high up to 30 \$/m$^2$ fabrication [48]. The calcium fluoride co-modified crystal powder synthesized by the hydrothermal method in PVDF has radiative cooling properties, which can reach below 5°C from ambient [80]. The 4A zeolite-based structure transformed to low-carnegieite $NaAlSiO_4$ by annealing at 800 °C achieved radiative cooling properties with 4°C below as compared to $TiO_2$ coated aluminum surface at noon [81].

## 4. Effect of environmental parameters

The performance of PDRC depends on ambient temperature, cloud cover, moisture, pollution and wind velocity. The effect of humidity was experimentally predicted by Bao et al. [78]. They showed that theoretically calculated below ambient temperature cannot be achieved experimentally due to the non-consideration of humidity and cloud fraction of atmosphere. However, a recalculation with consideration of humidity makes a good agreement between theoretical and experimental results, i.e., 3-5°C above the ambient temperature. Bartoli et al. [82] also experimented with and without a cloud for the selective radiator and found that cloud cover substantially reduces the cooling power. Torbjorn et al. [39] considered the effect of cloud cover and clear sky during the experiment on black radiator covered with pigmented foil to reflect the solar radiation and get 19 h of cooling in a day-night cycle in an arid location close to the equator. Bijarniya et al. [83] simulated the performance of PDRC integrated with conventional air conditioning systems at different climate conditions in the Indian subcontinent and depicted 35% of reduction in roof load for low humid climates. Whereas, Katramiz et al. [84] predicted a 32% reduction in window load in a semi-arid climate.

The effect of humidity and ambient temperature is used to show by a total water vapor column, which represents gaseous water in a vertical column (TWC) of the atmosphere. TWC of mid-latitude winter, subtropical winter and tropical climate vary from 1059.7 atm-cm, 3635.9 atm-cm and 5119.4 atm-cm, respectively, which lead to a decrease in atmospheric transmission 80% to less than 60% for tropical climate. Subsequently, it enhances the heat gain due to atmospheric radiation and decreases the cooling effect of radiative cooler [45]. An experiment used a combination of two-layer material of $SiO_2$–$TiO_2$ and $SiO_2$–$HfO_2$ conducted in Hong Kong with a humidity level of 55%, and both types of radiative coolers not showed any sub-ambient cooling. However, with shading $SiO_2$–$HfO_2$ achieves sub-ambient temperature due to its higher emissivity [3].

The high humidity or cloud cover blocks the atmospheric window in 8–13 µm range due to the presence of water vapor, which absorbs/emits in the specified atmospheric window, leads to radiative cooler nearly ineffective. To overcome humidity problem broadband emitting radiative cooler improves the performance during the daytime to some extent [45] and a numerically developed asymmetric electromagnetic transmission (AEMT) grating restores about 57% of cooling effect with a transmission ratio of 2. The AEMT is a theoretical suggestion that allows transmission from the radiative cooler and reflects incoming radiative energy at the same wavelength with varying transmission ratios. The AEMT was realized by many researchers, but it covers a narrow range of

wavelength or just at specific wavelength; the radiative cooling device requires broadband AEMT and was proposed theoretically as a periodic microstructure of inverted trapezoidal cross-section made up of Ag [85].

The effect of wind over a radiative cooler can be suppressed by a wind-shield and depends directly on change in wind velocity for daytime and nighttime radiative cooling. The sub-ambient radiative surface has a negative impact of wind and loss of cooling effect was observed; however, the above ambient surface can be further cooled by convection [86, 87].

The convective heat transfer [88] over a surface is given by,

$$P_{conv} = hA_r(T_{amb} - T_s) \tag{30}$$

Heat transfer coefficient, $h = 2.8 + 3.0u_a \tag{31}$

$u_a$, is the wind velocity. $A_r$ is the surface area of radiative cooler exposed to ambient. Pollution also has a negative effect on PDRC performance, such as particulate emission can absorb or emit the radiation leads to a decrease in cooling power; however, the pollution effect has not been studied. Finally, it can be concluded that higher atmospheric humidity, cloud cover, higher wind velocity and pollution degrade the PDRC performance.

## 5. Application and challenges

The radiative cooling can be utilized in both a passive way in which the cooler is directly attaching to the roof of a house or solar PV and an active way by circulating heat transfer fluid below to cooler for extracting cold energy. The heat transfer fluid is further coupled with the condenser of the power plant and air conditioning system, water cooling and space cooling systems. Active systems have user control and can utilize optimally; however, passive cooling systems are simpler in design and less control over desired cooling [89]. In this section, potential applications of radiative cooling are described in detail.

### 5.1. Water cooling

Zhao D et al. [90] designed and experimentally demonstrated a water cooling application, as shown in Fig. 4 and maintained 10.6°C below the ambient temperature, they build 13.5 m$^2$ radiative cooling area with module tilted 15° north which reduces incident solar flux, recorded a cooling power of 1296 W at night and 607 W at solar peak irradiance which correspond to 96 W/m$^2$ and 45 W/m$^2$ cooling flux respectively.

Goldstein et al. [91] used a radiative cooler for water cooling, 5°C below ambient temperature with an average flux of 40 W/m$^2$ with a system comprising radiative cooer surface, plate heat exchanger and insulating enclosure of Styrofoam.
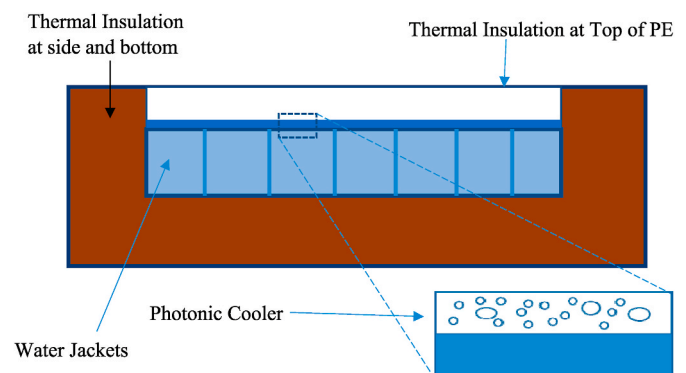


**Fig. 4.** Water cooling from a radiative cooler.

## 5.2. Space cooling

The energy requirements of a building including commercial and residential significantly high, nearly 40% of total energy consumption [1], and space cooling alone account for 12%, which can be diverted to radiative cooling due to available roof surface area and has the potential to reduce consumption of conventional energy resources [88]. Jeong et al. [92] simulated the performance of radiative cooler with emissivity unity in the atmospheric window and 0.1 elsewhere for space cooling systems. They build a 100 m$^2$ radiative cooler with microchannel back to it for the flow of water as heat transfer fluid and further utilized to cool the air for space cooling (Fig. 5). A drop of 10ºC in indoor air temperature was observed with a net cooling capacity of 1600 W, which has the potential to reduce 35% energy consumption by supporting conventional space cooling systems.

In another study, a radiative cooler made of copolymer mirror (3M vikiuiti ESR film) used for space cooling indirectly coupled with a conventional cooling system's condenser. By covering 60% of building rooftop areas with zero water loss building, an integrated radiative cooling system reduced the electricity demand by 21% [91]. Numerically with a multilayer structure PDRC, 10% of available rooftop space can overcome 35% of air conditioning needed in a building during the hottest hours of a day [13].

## 5.3. Power plant condenser cooling

A condenser of power plant need to forcefully cool and water is required in the cooling tower as well for circulation in a heat exchanger; certain power plants like concentrated solar power (CSP) plant operate on dry cooling due to scarcity of cooling water due to location specific and operates on compromised thermal cycle efficiency. A generalized study of a covered pond with radiative cooler revealed that 150 W/m$^2$ flux could be achieved without loss of water [93], these study further validated by experiment and resulted in an average night time cooling power of this pond limited to 50 W/m$^2$ due to less development in the material that time [94]. However, for a CSP operating on the $CO_2$ supercritical cycle at 550 ºC can be improved in 5% net output over an air-cooled system by integration with 14 m$^2$/kW$_e$ capacity radiative cooler [95]. Sarkar analyzed the supercritical $CO_2$ cycle for power plants and found that the effect of minimum operating temperature is dominated on optimum pressure ratio than maximum operating temperature [96], which again signifies the utilization of radiative cooler coupled to the condenser to get desired minimum temperature of the cycle. The area requirement of the radiative cooled thermal power plant is higher to achieve condenser cooling alone by radiative cooler, but nighttime radiative cooling is extended opportunity to use the same area of concentrating mirrors and potential to achieve 90% of requirement [97].

Zhang et al. supplemented the air-cooled condenser of a thermoelectric power plant with radiative cooling panels. They have used a thermal storage tank and piping systems as shown in Fig. 6 to supply the cold heat transfer fluid to condenser and optimized the piping system
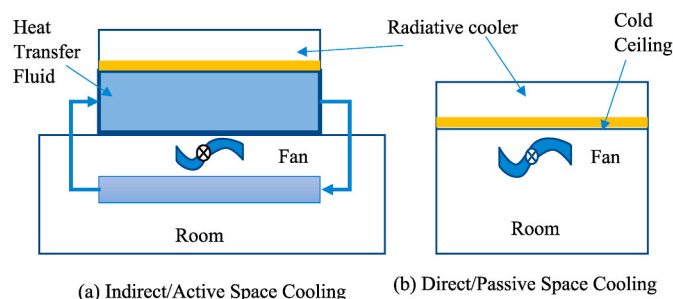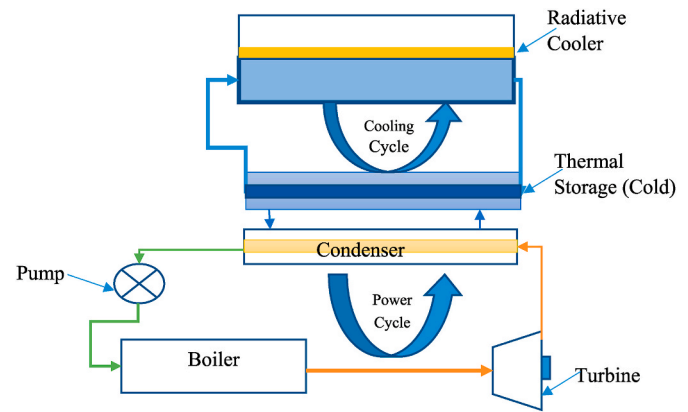


**Fig. 6.** Layout of condenser integrated with radiative cooler.

with a T-shape network and get a 4096 kWh$_{th}$/day cooling effect with a pump energy consumption of 11 kWh/day [98].

## 5.4. Other applications

Lee et al. [55] and Tong et al. [99] developed radiative cooling material for wearable electronic devices with different colors for aesthetic dominant applications. The outdoor applications and things such as automobiles, clothing, and buildings chosen based on their color to some extent. For the same reason, with the help of meta-material radiative cooling can be achieved, and a temperature difference of 47.6 ºC noticed [51]. Slauch et al. theoretically proposed a photonic mirror for solar photovoltaic cells to improve the energy yield by 3.7%. The temperature of the solar PV cell rises due to sub-bandgap photon energy absorption and gets converted into heat, which acts as a parasitic heat gain. A photonic mirror blocks sub-bandgap photon which accounts for nearly 19% for Si module (bandgap of 1.1 eV) and transmits useful radiation to the solar cell, and they constructed a thin film of the photonic mirror with an optimized thickness of $SiO_2$, $TiO_2$, $Si_3N_4$, and $Al_2O_3$ [100]. 1ºC temperature rise of the solar cells over 25ºC reduces 0.45% relative efficiency, sub-band-gap and UV spectra absorption are responsible for heat gain in solar cells, so simultaneously, three operations happen for photonic structure transmission of useful spectra, a reflection of UV and NIR spectra and emission of MIR spectra. The alternating layers of $Al_2O_3$/SiN/$TiO_2$/SiN and $SiO_2$ at the bottom of the selective radiative cooler for solar cells and lowered the solar cell temperature by 5.7ºC [101]. However, the nitride-based solar cell is also in the research process that can operate at elevated temperature efficiently [26].

The spacecraft thermal control is critical due to too large variation in temperature. So, there is a need for temperature control at a suitable temperature, where radiative cooling and heat gain have balances; this usually achieved at elevated temperature. Taylor et al. [102] suggested a switchable coating of $VO_2$ based dielectric metallic structure having the property of asymmetric Fabry-Perot emitter. These structures, as shown in Fig. 3, have high reflectance of IR spectrum 5–25 μm below 341 K and emissive above it. Similarly, Kort-Kamp et al. simulated the phase change photonic structure for summer and winter thermal adjustment by IR emissive and Solar absorbing spectrum, respectively [103]. Sun et al. proposed an aluminum-doped zinc oxide (AZO) as an alternative of traditional rigid quartz tiles for cooling of spacecraft with lower weight and launch costs; they found similar results for fabricated model and FDTD simulation [104]. Hsu et al. observed the reduction of indoor energy requirement by 20% by lowering the temperature of the skin and emitting higher through radiative cooling, which is possible from nanoPE microfibers, which are opaque for visible and transparent for IR [67,70]. In the zero energy building application, Hu et al. [105] proposed a combined photothermal and radiative cooling module for heating and cooling in the day time and night time, respectively. Their



(a) Indirect/Active Space Cooling     (b) Direct/Passive Space Cooling

**Fig. 5.** Space cooling using radiative cooler.

module consists of solar selective absorber coating and glazing of ultra-white glass separated by air tunnel to carry thermal load used for photothermal daytime heating and nighttime radiative cooling, respectively.

*5.5. Challenges*

From the above literature review, several challenges can be identified related to applications. Cost, optimized design, operational safety and durability of the PDRC material are the key challenges before implementation. Low cost is an important criterion, especially for developed countries like India. Low-cost device is related to low-cost material and easy availability as well as the manufacturing process. The durability or stability study of PDRC materials has not been conducted yet. The management/disposal of waste materials is another challenge. Low energy density and humidity of atmosphere are two challenges for the radiative cooling system. For an active system, low energy density means the circulation of heat transfer fluid to a large area and needs significant pumping power [90]. This can certainly to be true that the life cycle of major developed materials is very short, which needs to enhance and can be done through polymers and plastic-like materials [40]. Radiative cooler integrated with roof increases the energy demand due to higher heating energy and visual discomfort by specular reflection. Due to dirt deposition on open radiative cooling surface albedo/reflectivity decreases very fast in the initial phase, this can be overcome by manual soap washing; however, a self-cleaning material development still required [106]. Cloud and high humidity will degrade the performance of radiative cooler and that's why the performance of this cooler is not good in the coastal region. A study by Bijarniya et al. [83] showed that the PDRC is not so effective for the cities of high humid or coastal zone cities. It is a big challenge as many populated cities in the world are in the coastal region. Minimize the convective heat transfer is also another challenge for implementation due to relatively higher wind speed in the coastal zone. Frost formation is another disadvantageous thing related to radiative cooling, frost formation on car window due to IR emission is common in cold weather. Heating is one way to remove the frost; however, low emitting material $SnO_2$ coating eliminates the need for heating [107]. An important disadvantage of PDRC is that it can only reduce temperature and hence it is not fit for most air-conditioning systems as both temperature, as well as humidity control, is required.

## 6. Conclusions and future scope

In this review, passive daytime radiative cooling is extensively reviewed with fundamentals of electromagnetic wave and material interaction, energy analysis, categorization based on material and fabrication, the environmental effect on performance, applications and associated challenges. From literature, it is revealed that a number of potential metamaterials have radiative cooling properties and optimized material design is possible based on electromagnetic wave interaction. The focus point of all developed material structures is to suppress the solar irradiation and enhance emissivity in the atmospheric window only. Three major potential categories are identified, such as layered medium, randomly distributed, and porous polymer structure-proved technology to achieve sub-ambient during daytime or at peak irradiance. Fabrication of these radiative coolers owns a wide range of techniques from e beam evaporation through sputtering to a simple spray coating or chemical solution deposition. It is also found out that materials have a negligible extinction coefficient in the solar spectrum, with a significant difference in the real part of the refractive index and extinction peaks in the atmospheric window are highly suitable to achieve radiative cooling. The effect of the operational parameter is described in energy analysis and environmental factors responsible for altering the performance identified as humidity, cloud fraction, wind velocity, etc. Environmental parameters have found a significant

influence on performance. Several attempts on the application of radiative cooler are reported by many researchers; however, the short life cycle challenges the field use of this technology. The domain of applications of radiative cooler tested in literature is water cooling, space cooling, condenser cooling in a hybrid system, solar PV cell cooling, aircraft cooling, human body cooling through wearable's, automobiles and electronic devices with aesthetics values. Finally, some challenges associated with the radiative cooler are described in brief. Despite some challenges, the radiative cooling technology has lots of futuristic application opportunities in view of environmental protection, water and energy securities. Based on the above review and discussed challenges, some suggestions for further research can be drawn as follows:

➢ Optimized material design based on electromagnetic wave interaction is needed for required surface emissive properties of the passive radiative cooler
➢ There is a scope for development of cost-effective and easy to fabricate daytime radiative cooler. Random and porous polymer structure has the potential for further research at a low cost.
➢ The life cycle and stability of radiative cooler should be studied because of radiative cooler have the exposure of sunlight, dust, rain, and pollution, which derate the exposed surfaces over time passes.
➢ Despite a large number of applications (space cooling, water cooling, PV panel cooling, wearable, etc.) proved, one most prominent economic feasible application should be researched.
➢ Passive radiative cooling is suitable for low cold energy flux-based applications with 24 h-long requirement and that could be selected for further research along with cold energy storage.
➢ The yearlong experiment to prove material stability, seasonality and economic feasibility should be investigated, as the literature reported till now have maximum 2–3 days of continuous 24 h cycle experimental results.
➢ As environmental parameters have a strong influence, there is a scope for climate-based techno-socio-economic study and further research/technique to reduce the effect, especially for the humid and windy climate.

## Declaration of competing interest

The authors declare that they have no known competing financial interests or personal relationships that could have appeared to influence the work reported in this paper.

## Nomenclature

| | |
|---|---|
| a | Particle radius |
| AEMT | Asymmetric electromagnetic wave transmission |
| B | Magnetic displacement field |
| c | Speed of light |
| CRP | Cool Roof Paints |
| D | Electric displacement field |
| E | Electric field |
| FDTD | Finite difference time domain |
| h | Plank's constant, heat transfer coefficient |
| H | Magnetic field |
| I | Irradiation |
| k | Stephan Boltzmann's constant |
| M | Magnetic polarization |
| MIM | Metal insulator metal |
| MIR | Mid Infrared |
| NIR | Near infrared |
| P | Power, Electric polarization |
| PCSUVA | Photonic Crystal Structured UV curable Adhesive |
| PDMS | Polydimethylsiloxane |
| PDRC | Passive Daytime Radiative Cooling |
| PET | Polyethylene Terephthalate |

| | |
|---|---|
| PV | Photovoltaic |
| RCWA | Rigorous coupled wave analysis |
| TMM | Transfer matrix method |
| u | velocity |
| λ | Wavelength |
| μ | Magnetic permeability |
| ε | Electric permittivity |

## References

[1] Pérez-Lombard L, Ortiz J, Pout C. A review on buildings energy consumption information. Energy Build 2008;40:394–8. https://doi.org/10.1016/j.enbuild.2007.03.007.

[2] Zhao B, Hu M, Ao X, Xuan Q, Pei G. Spectrally selective approaches for passive cooling of solar cells : a review. Appl Energy 2020;262:114548.

[3] Jeong SY, Tso CY, Ha J, Wong YM, Chao CYH, Huang B, et al. Field investigation of a photonic multi-layered TiO2 passive radiative cooler in sub-tropical climate. Renew Energy 2020;146:44–55. https://doi.org/10.1016/j.renene.2019.06.119.

[4] Trombe F. Perspectives sur l'utilisation des rayonnements solaires et terrestres dans certainesre regions du monde. Rev Gen Therm 1967;6:1285–314.

[5] Catalanotti S, Cuomo V, Piro G, Ruggi D, Silvestrini V, Troise G. The radiative cooling of selective surfaces. Sol Energy 1975;17:83–9.

[6] Eriksson TS, Lushiku EM, Granqvist CG. Materials for radiative cooling to low temperature. Sol Energy Mater 1984;11:149–61.

[7] Eriksson TS, Jiang SJ, Granqvist CG. Surface coatings for radiative cooling applications: silicon dioxide and silicon nitride made by reactive rf-sputtering. Sol Energy Mater 1985;12:319–25.

[8] Granqvist CG, Hjortsberg A. Surfaces for radiative cooling: silicon monoxide films on aluminum. Appl Phys Lett 1980;36:139–41. https://doi.org/10.1063/1.91406.

[9] Ben-Shalom A, Barzilai B, Cabib D, Devir AD, Lipson SG, Oppenheim UP. Sky radiance at wavelengths between 7 and 14 μm: measurement, calculation, and comparison with lowtran-4 predictions. Appl Optic 1980;19:838.

[10] Berdhal P. Radiative cooling with MgO and/or LiFLayers. Appl Optic 1984;23:370–2. https://doi.org/10.1364/AO.28.003268.

[11] Hori M, Aoki T, Tanikawa T, Motoyoshi H, Hachikubo A, Sugiura K, et al. In-situ measured spectral directional emissivity of snow and ice in the 8-14 μm atmospheric window. Remote Sens Environ 2006;100:486–502. https://doi.org/10.1016/j.rse.2005.11.001.

[12] Gentle AR, Smith GB. Radiative heat pumping from the Earth using surface phonon resonant nanoparticles. Nano Lett 2010;10:373–9. https://doi.org/10.1021/nl903271d.

[13] Rephaeli E, Raman A, Fan S. Ultrabroadband photonic structures to achieve high-performance daytime radiative cooling. Nano Lett 2013;13:1457–61. https://doi.org/10.1021/nl4004283.

[14] Raman AP, Anoma MA, Zhu L, Rephaeli E, Fan S. Passive radiative cooling below ambient air temperature under direct sunlight. Nature 2014;515:540–4.

[15] Al-Obaidi KM, Ismail M, Abdul Rahman AM. Passive cooling techniques through reflective and radiative roofs in tropical houses in Southeast Asia: a literature review. Front Archit Res 2014;3:283–97. https://doi.org/10.1016/j.foar.2014.06.002.

[16] Hossain MM, Gu M. Radiative cooling: principles, progress, and potentials. Adv Sci 2016;3:1500360. https://doi.org/10.1002/advs.201500360.

[17] Tan Y, Liu B, Shen S, Yu Z. Enhancing radiative energy transfer through thermal extraction. Nanophotonics 2016;5:22–30. https://doi.org/10.1515/nanoph-2016-0008.

[18] Vall S, Castell A. Radiative cooling as low-grade energy source: a literature review. Renew Sustain Energy Rev 2017;77:803–20. https://doi.org/10.1016/j.rser.2017.04.010.

[19] Sun X, Sun Y, Zhou Z, Alam MA, Bermel P. Radiative sky cooling: fundamental physics, materials, structures, and applications. Nanophotonics 2017;6:997–1015.

[20] Family R, Mengüç MP. Materials for radiative cooling: a review. Procedia Environ Sci 2017;38:752–9. https://doi.org/10.1016/j.proenv.2017.03.158.

[21] Santamouris M, Feng J. Recent progress in daytime radiative Cooling : is it the air conditioner of the Future ? Buildings 2018;8:168. https://doi.org/10.3390/buildings8120168.

[22] Zhao B, Hu M, Ao X, Chen N, Pei G. Radiative cooling: a review of fundamentals, materials, applications, and prospects. Appl Energy 2019;236:489–513.

[23] Zhao D, Aili A, Zhai Y, Xu S, Tan G, Yin X, et al. Radiative sky cooling: fundamental principles, materials, and applications. Appl Phys Rev 2019;6. https://doi.org/10.1063/1.5087281.

[24] Ko B, Lee D, Badloe T, Rho J. Metamaterial-based radiative cooling: towards energy-free all-day cooling. Energies 2019;12:1–14. https://doi.org/10.3390/en12010089.

[25] Boriskina SV, Weinstein LA, Tong JK, Hsu W, Chen G. Hybrid optical − thermal antennas for enhanced light focusing and local temperature control. ACS Photonics 2016;3:1714–22. https://doi.org/10.1021/acsphotonics.6b00374.

[26] Huang X, Li W, Fu H, Li D, Zhang C, Chen H, et al. High-temperature polarization-free III-nitride solar cells with self-cooling effects. ACS Photonics 2019;6:2096–103. https://doi.org/10.1021/acsphotonics.9b00655.

[27] Bethune DS. Optical harmonic generation and mixing in multilayer media: analysis using optical transfer matrix techniques. J Opt Soc Am B 1989;6:910–6.

[28] Katsidis CC, Siapkas DI. General transfer-matrix method for optical multilayer systems with coherent, partially coherent, and incoherent interference. Appl Optic 2002;41:3978–87.

[29] Moharam MG. Coupled -wave analysis of two -dimensional dielectric gratings. Hologr Opt Des Appl 1988;883:8–11.

[30] Yee KS. Numerical solution of initial boundary value problems involving Maxwell's equations in isotropic media. IEEE Trans Antenn Propag 1966;14:302–7. AP.

[31] Weber MF, Stover CA, Gilbert LR, Nevitt TJ, Ouderkirk AJ. Giant birefringent optics in multilayer polymer mirrors. Science 2000;287:2451–6. 80-.

[32] Zhai Y, Ma Y, David SN, Zhao D, Lou R, Tan G, et al. Scalable-manufactured randomized glass-polymer hybrid metamaterial for daytime radiative cooling. Science 2017;355:1062–6. https://doi.org/10.1126/science.aai7899. 80-.

[33] Tikhonravov AV, Trubetskov MK, Amotchkina TV. Application of constrained optimization to the design of quasi-rugate optical coatings. Appl Optic 1996;35:5493–508. https://doi.org/10.1364/AO.47.005103.

[34] Shi Y, Li W, Raman A, Fan S. Optimization of multilayer optical films with a memetic algorithm and mixed integer programming. ACS Photonics 2018;5:684–91.

[35] Zaman MA. Photonic radiative cooler optimization using Taguchi's method. Int J Therm Sci 2019;144:21–6. https://doi.org/10.1016/j.ijthermalsci.2019.05.019.

[36] Niklasson GA, Eriksson TS. Radiative cooling with pigmented polyethylene foils. SPIE. Opt Mater Technol Energy Effic Sol Energy Convers VII 1988;1016:89–99.

[37] Dickmann J, Hurtado CBR, Nawrodt R, Kroker S. Influence of polarization and material on Brownian thermal noise of binary grating reflectors. Phys Lett 2018;382:2275–81. https://doi.org/10.1016/j.physleta.2017.07.006.

[38] Jonsson JC, Karlsson L, Nostell P, Niklasson GA, Smith GB. Angle-dependent light scattering in materials with controlled diffuse solar optical properties. Sol Energy Mater Sol Cells 2004;84:427–39. https://doi.org/10.1016/j.solmat.2004.02.048.

[39] Nilsson TMJ, Niklasson GA. Radiative cooling during the day: simulations and experiments on pigmented polyethylene cover foils. Sol Energy Mater Sol Cells 1995;37:93–118. https://doi.org/10.1016/0927-0248(94)00200-2.

[40] Mandal J, Fu Y, Overvig AC, Jia M, Sun K, Shi NN, et al. Hierarchically porous polymer coatings for highly efficient passive daytime radiative cooling. Science 2018;362:315–9. https://doi.org/10.1126/science.aat9513. 80-.

[41] Dilmac S, Tekin A. Radiative properties of polymer coatings from the point of view of energy conservation. Energy Build 1992;19:87–92.

[42] Kobayashi M, Tashiro K, Tadokoro H. Molecular vibrations of three crystal forms of poly(vinylidene fluoride). Macromolecules 1975;8:158–71.

[43] Gentle AR, Smith GB. A subambient open roof surface under the mid-summer sun. Adv Sci 2015;2:1500119. https://doi.org/10.1002/advs.201500119.

[44] Chen Z, Zhu L, Raman A, Fan S. Radiative cooling to deep sub-freezing temperatures through a 24-h day-night cycle. Nat Commun 2016;7:1–5. https://doi.org/10.1038/ncomms13729.

[45] Han D, Ng BF, Wan MP. Preliminary study of passive radiative cooling under Singapore's tropical climate. Sol Energy Mater Sol Cells 2020;206:110270.

[46] Yuan H, Yang C, Zheng X, Mu W, Wag Z, Yuan W, et al. Effective , angle-independent radiative cooler based on one-dimensional photonic crystal. Optic Express 2018;26:27885–93.

[47] Wu D, Liu C, Xu Z, Liu Y, Yu Z, Yu L, et al. The design of ultra-broadband selective near-perfect absorber based on photonic structures to achieve near-ideal daytime radiative cooling. Mater Des 2018;139:104–11. https://doi.org/10.1016/j.matdes.2017.10.077.

[48] Ao X, Hu M, Zhao B, Chen N, Pei G, Zou C. Preliminary experimental study of a specular and a diffuse surface for daytime radiative cooling. Sol Energy Mater Sol Cells 2019;191:290–6. https://doi.org/10.1016/j.solmat.2018.11.032.

[49] Atiganyanun S, Plumley JB, Han SJ, Hsu K, Cytrynbaum J, Peng TL, et al. Effective radiative cooling by paint-format microsphere-based photonic random media. ACS Photonics 2018;5:1181–7. https://doi.org/10.1021/acsphotonics.7b01492.

[50] Blake TA, Johnson TJ, Tonkyn RG, Forland BM, Myers TL, Brauer CS, et al. Quantitative total and diffuse reflectance laboratory measurements for remote , standoff , and point sensing. Proc SPIE 2014;9073:1–10. https://doi.org/10.1117/12.2054116.

[51] Li W, Shi Y, Chen Z, Fan S. Photonic thermal management of coloured objects. Nat Commun 2018;9:4240. https://doi.org/10.1038/s41467-018-06535-0.

[52] Catrysse PB, Song AY, Fan S. Photonic structure textile design for localized thermal cooling based on a fiber blending scheme. ACS Photonics 2016;3:2420–6.

[53] long Kou J, Jurado Z, Chen Z, Fan S, Minnich AJ. Daytime radiative cooling using near-black infrared emitters. ACS Photonics 2017;4:626–30.

[54] Wu J-Y, Gong Y-Z, Huang P-R, Ma G-J, Dai Q-F. Diurnal cooling for continuous thermal sources under direct subtropical sunlight produced by quasi-Cantor structure. Chin Phys B 2017;26:104201. https://doi.org/10.1088/1674-1056/26/10/104201.

[55] Lee GJ, Kim YJ, Kim HM, Yoo YJ, Song YM. Colored , daytime radiative coolers with thin-film resonators for aesthetic purposes. Adv Opt Mater 2018;6:1800707.

[56] Gao M, Han X, Chen F, Zhou W, Liu P, Shan Y, et al. Approach to fabricating high-performance cooler with near-ideal emissive spectrum for above-ambient air temperature radiative cooling. Sol Energy Mater Sol Cells 2019;200:110013.

[57] Cunha NF, Al-rjoub A, Rebouta L, Vieira LG, Lanceros-mendez S. Multilayer passive radiative selective cooling coating based on Al/SiO2/SiNx/SiO2/TiO2/SiO2 prepared by dc magnetron sputtering. Thin Solid Films 2020;694:137736.

[58] Demiryont H. Optical properties of SiO2 -TiO2 composite films. Appl Optic 1985;24:2647–50.

[59] Chao S, Chang C, Chen J. TiO2 -SiO2 mixed films prepared by the fast alternating sputter method. Appl Optic 1991;30:3233–7.

[60] Schulz LG. The optical constants of silver, gold, copper, and aluminum. J Opt Soc Am 1954;44:357–62.

[61] Pech-may NW, Retsch M. Nanoscale Advances a broadband angle selective low-pass filter. Nanoscale Adv 2020;2:249–55. https://doi.org/10.1039/c9na00557a.

[62] Shahsafi A, Joe G, Brandt S, Shneidman AV, Stanisic N, Xiao Y, et al. Wide-angle spectrally selective absorbers and thermal emitters based on inverse opals. ACS Photonics 2019;6:2607–11. https://doi.org/10.1021/acsphotonics.9b00922.

[63] Fan J, Fu C, Fu T. Yttria-stabilized zirconia coating for passive daytime radiative cooling in humid environment. Appl Therm Eng 2020;165:114585.

[64] Ma H, Yao K, Dou S, Xiao M, Dai M, Wang L, et al. Multilayered SiO2/Si3N4 photonic emitter to achieve high-performance all-day radiative cooling. Sol Energy Mater Sol Cells 2020;212:110584. https://doi.org/10.1016/j.solmat.2020.110584.

[65] Yang Y, Long L, Meng S, Denisuk N, Chen G, Wang L, et al. Bulk material based selective infrared emitter for sub-ambient daytime radiative cooling. Sol Energy Mater Sol Cells 2020;211:110548. https://doi.org/10.1016/j.solmat.2020.110548.

[66] Zhou L, Song H, Liang J, Singer M, Zhou M, Stegenburgs E, et al. A polydimethylsiloxane-coated metal structure for all-day radiative cooling. Nat Sustain 2019;2:718–24. https://doi.org/10.1038/s41893-019-0348-5.

[67] Peng Y, Chen J, Song AY, Catrysse PB, Hsu PC, Cai L, et al. Nanoporous polyethylene microfibres for large-scale radiative cooling fabric. Nat Sustain 2018;1:105–12. https://doi.org/10.1038/s41893-018-0023-2.

[68] Li T, Zhai Y, He S, Gan W, Wei Z, Heidarinejad M, et al. A radiative cooling structural material. Science 2019;364:760–3. https://doi.org/10.1126/science.aau9101.

[69] Wang X, Liu X, Li Z, Zhang H, Yang Z, Zhou H, et al. Scalable flexible hybrid membranes with photonic structures for daytime radiative cooling. Adv Funct Mater 2020;30:1907562. https://doi.org/10.1002/adfm.201907562.

[70] Hsu PC, Song AY, Catrysse PB, Liu C, Peng Y, Xie J, et al. Radiative human body cooling by nanoporous polyethylene textile. Science 2016;353:1019–23. https://doi.org/10.1126/science.aaf5471. 80-.

[71] Zhang H, Ly KCS, Liu X, Chen Z, Yan M, Wu Z, et al. Biologically inspired flexible photonic films for efficient passive radiative cooling. Proc Natl Acad Sci Unit States Am 2020;117:14657–66.

[72] Jeong SY, Tso CY, Wong YM, Chao CYH, Huang B. Daytime passive radiative cooling by ultra emissive bio-inspired polymeric surface. Sol Energy Mater Sol Cells 2020;206:110296. https://doi.org/10.1016/j.solmat.2019.110296.

[73] Engelhard T, Jones ED, Viney I, Mastai Y, Hodes G. Deposition of tellurium films by decomposition of electrochemically-generated H2Te: application to radiative cooling devices. Thin Solid Films 2000;370:101–5. https://doi.org/10.1016/S0040-6090(00)00942-1.

[74] Dobson KD, Hodes G, Mastai Y. Thin semiconductor films for radiative cooling applications. Sol Energy Mater Sol Cells 2003;80:283–96. https://doi.org/10.1016/j.solmat.2003.06.007.

[75] Kitamura R, Pilon L, Jonasz M. Optical constants of silica glass from extreme ultraviolet to far infrared at near room temperature. Appl Optic 2007;46:8118–33. https://doi.org/10.1364/AO.46.008118.

[76] Zhong M, Fu W, Da W, Su D. Study on preparation and near-infrared reflective properties of NaZnPO4. Adv Mater Res 2012;399–401:1289–93. https://doi.org/10.4028/www.scientific.net/AMR.399-401.1289.

[77] Atiganyanun S, Zhou M, Abudayyeh OK, Han SM, Han SE. Control of randomness in microsphere-based photonic crystals assembled by Langmuir-blodgett process. Langmuir 2017;33:13783–9. https://doi.org/10.1021/acs.langmuir.7b03060.

[78] Bao H, Yan C, Wang B, Fang X, Zhao CY, Ruan X. Double-layer nanoparticle-based coatings for efficient terrestrial radiative cooling. Sol Energy Mater Sol Cells 2017;168:78–84. https://doi.org/10.1016/j.solmat.2017.04.020.

[79] Huang Z, Ruan X. Nanoparticle embedded double-layer coating for daytime radiative cooling. Int J Heat Mass Tran 2017;104:890–6.

[80] Huang X, Liu D, Li N, Wang J, Zhang Z, Zhong M. Single novel Ca0.5Mg10.5 (HPO3)8(OH)3F3 coating for efficient passive cooling in the natural environment. Sol Energy 2020;202:164–70. https://doi.org/10.1016/j.solener.2020.03.103.

[81] Lv C, Zu M, Xie D, Yan F, Li M, Cheng H. 4A zeolite based daytime passive radiative cooling material. Infrared Phys Technol 2020;107:103342.

[82] Bartoli B, Catalanotti S, Coluzzi B, Cuomo V, Silvestrini V, Troise G. Nocturnal and diurnal performances of selective radiators. Appl Energy 1977;3:267–86. https://doi.org/10.1016/0306-2619(77)90015-0.

[83] Bijarniya JP, Sarkar J, Maiti P. Environmental effect on the performance of passive daytime photonic radiative cooling and building energy-saving potential. J Clean Prod 2020;274:123119. https://doi.org/10.1016/j.jclepro.2020.123119.

[84] Katramiz E, Ghaddar N, Ghali K. Daytime radiative cooling : to what extent it enhances office cooling system performance in comparison to night cooling in

semi-arid climate ? J Build Eng 2020;28:101020. https://doi.org/10.1016/j.jobe.2019.101020.

[85] Wong RYM, Tso CY, Chao CYH, Huang B, Wan MP. Ultra-broadband asymmetric transmission metallic gratings for subtropical passive daytime radiative cooling. Sol Energy Mater Sol Cells 2018;186:330–9. https://doi.org/10.1016/j.solmat.2018.07.002.

[86] Hu M, Zhao B, Li J, Wang Y, Pei G. Preliminary thermal analysis of a combined photovoltaic–photothermic–nocturnal radiative cooling system. Energy 2017;137:419–30. https://doi.org/10.1016/j.energy.2017.03.075.

[87] Golaka A, Exell RHB. An investigation into the use of a wind shield to reduce the convective heat flux to a nocturnal radiative cooling surface. Renew Energy 2007;32:593–608. https://doi.org/10.1016/j.renene.2006.03.007.

[88] Gang P, Huide F, Tao Z, Jie J. A numerical and experimental study on a heat pipe PV/T system. Sol Energy 2011;85:911–21. https://doi.org/10.1016/j.solener.2011.02.006.

[89] Lu X, Xu P, Wang H, Yang T, Hou J. Cooling potential and applications prospects of passive radiative cooling in buildings: the current state-of-the-art. Renew Sustain Energy Rev 2016;65:1079–97. https://doi.org/10.1016/j.rser.2016.07.058.

[90] Zhao D, Aili A, Zhai Y, Lu J, Kidd D, Tan G, et al. Subambient cooling of water: toward real-world applications of daytime radiative cooling. Joule 2019;3:111–23. https://doi.org/10.1016/j.joule.2018.10.006.

[91] Goldstein EA, Raman AP, Fan S. Sub-ambient non-evaporative fluid cooling with the sky. Nat Energy 2017;2:1–7. https://doi.org/10.1038/nenergy.2017.143.

[92] Jeong SY, Tso CY, Zouagui M, Wong YM, Chao CYH. A numerical study of daytime passive radiative coolers for space cooling in buildings. Build Simul 2018;11:1011–28.

[93] Olwi IA, Sabbagh JA, Khalifa AMA. Mathematical modeling of passive dry cooling for power plants in arid land. Sol Energy 1992;48:279–86.

[94] Sabbagh JA, Khalifa AMA, Olwi IA. Development of passive dry cooling system for power plants in arid land. Sol Energy 1993;51:431–47.

[95] Zeyghami M, Khalili F. Performance improvement of dry cooled advanced concentrating solar power plants using daytime radiative cooling. Energy Convers Manag 2015;106:10–20. https://doi.org/10.1016/j.enconman.2015.09.016.

[96] Sarkar J. Second law analysis of supercritical CO2 recompression Brayton cycle. Energy 2009;34:1172–8. https://doi.org/10.1016/j.energy.2009.04.030.

[97] Dyreson A, Miller F. Night sky cooling for concentrating solar power plants. Appl Energy 2016;180:276–86. https://doi.org/10.1016/j.apenergy.2016.07.118.

[98] Zhang K, Zhao D, Zhai Y, Yin X, Yang R, Tan G. Modelling study of the low-pump-power demand constructal T-shaped pipe network for a large scale radiative cooled-cold storage system. Appl Therm Eng 2017;127:1564–73. https://doi.org/10.1016/j.applthermaleng.2017.08.131.

[99] Tong JK, Huang X, Boriskina SV, Loomis J, Xu Y, Chen G. Infrared-transparent visible-opaque fabrics for wearable personal thermal management. ACS Photonics 2015;2:769–78. https://doi.org/10.1021/acsphotonics.5b00140.

[100] Slauch IM, Deceglie MG, Silverman TJ, Ferry VE. Spectrally selective mirrors with combined optical and thermal bene fi t for photovoltaic module thermal management. ACS Photonics 2018;5:1528–38. https://doi.org/10.1021/acsphotonics.7b01586.

[101] Li W, Shi Y, Chen K, Zhu L, Fan S. A comprehensive photonic approach for solar cell cooling. ACS Photonics 2017;4:774–82. https://doi.org/10.1021/acsphotonics.7b00089.

[102] Taylor S, Yang Y, Wang L. Vanadium dioxide based Fabry-Perot emitter for dynamic radiative cooling applications. J Quant Spectrosc Radiat Transf 2017;197:76–83. https://doi.org/10.1016/j.jqsrt.2017.01.014.

[103] Kort-kamp WJM, Kramadhati S, Azad AK, Reiten MT, Dalvit DAR. Passive radiative "thermostat" enabled by phase-change photonic nanostructures. ACS Photonics 2018;5:4554–60. https://doi.org/10.1021/acsphotonics.8b01026.

[104] Sun K, Riedel CA, Wang Y, Urbani A, Simeoni M, Mengali S, et al. Metasurface optical solar refl ectors using AZO transparent conducting oxides for radiative cooling of spacecraft. ACS Photonics 2018;5:495–501. https://doi.org/10.1021/acsphotonics.7b00991.

[105] Hu M, Zhao B, Ao X, Chen N, Cao J, Wang Q, et al. Feasibility research on a double-covered hybrid photo-thermal and radiative sky cooling module. Sol Energy 2020;197:332–43. https://doi.org/10.1016/j.solener.2020.01.022.

[106] Bretz SE, Akbari H. Long-term performance of high-albedo roof coatings. Energy Build 1997;25:159–67. https://doi.org/10.1016/s0378-7788(96)01005-5.

[107] Hamberg I, Svensson JSEM, Eriksson TS, Granqvist C-G, Arrenius P, Norin F. Radiative cooling and frost formation on surfaces with different thermal emittance: theoretical analysis and practical experience. Appl Optic 1987;26:2131–6. https://doi.org/10.1364/ao.26.002131.